INL/RPT-22-69810
Revision 0

# Margin to Onset of Nucleate Boiling studies for MITR and NBSR Design Demonstration Experiments

October 2022

Mauricio E. Tano. Theron Marshall

Idaho National Laboratory

INL is a U.S. Department of Energy National Laboratory
operated by Battelle Energy Alliance, LLC

**DISCLAIMER**

This information was prepared as an account of work sponsored by an agency of the U.S. Government. Neither the U.S. Government nor any agency thereof, nor any of their employees, makes any warranty, expressed or implied, or assumes any legal liability or responsibility for the accuracy, completeness, or usefulness, of any information, apparatus, product, or process disclosed, or represents that its use would not infringe privately owned rights. References herein to any specific commercial product, process, or service by trade name, trade mark, manufacturer, or otherwise, does not necessarily constitute or imply its endorsement, recommendation, or favoring by the U.S. Government or any agency thereof. The views and opinions of authors expressed herein do not necessarily state or reflect those of the U.S. Government or any agency thereof.

INL/RPT-22-69810
Revision 0

# Margin to Onset of Nucleate Boiling studies for MITR and NBSR Design Demonstration Experiments

Mauricio E. Tano

October 2022

Idaho National Laboratory
Nuclear Science & Technology
Idaho Falls, Idaho 83415

http://www.inl.gov

Prepared for the
U.S. Department of Energy
Office of Nuclear Energy
Under DOE Idaho Operations Office
Contract DE-AC07-05ID14517

# CONTENTS

## FIGURES

# TABLES

# ACRONYMS

| | |
|---|---|
| BOC | Beginning of Cycle |
| BR2 | Belgian Reactor 2 |
| CAD | Computer-Aided Design |
| DDE | Design Demonstration Element |
| HEU | High Enriched Uranium |
| MITR | Massachusetts Institute of Technology Reactor |
| NBSR | National Bureau of Standards Reactor |
| ONB | Onset of Nucleate Boiling |
| RELAP | Reactor Excursion and Leakage Analysis Program |
| U-10Mo | Uranium-10 wt% Molybdenum |
| USHPRR | United State High Performance Research Reactor |

*Page intentionally left blank*

# 1. INTRODUCTION

## 1.1 OBJECTIVE

The United State High Performance Research Reactor (USHPRR) program aims to eliminate more than 200kg of High Enriched Uranium (HEU) from commerce annually by converting five U.S. high-performance research reactors and one associated critical assembly to Low Enriched Uranium (LEU) fuel using a high-density alloy of uranium-10 wt% molybdenum (U-10Mo). The Massachusetts Institute of Technology Reactor (MITR) and the National Bureau of Standards Reactor (NBSR) are two of five research reactors selected for this program. Previous studies have addressed the thermal-hydraulics performance of the fuel Design Demonstration Elements (DDE) for these reactors under conservative assumptions in the Belgian Reactor (BR)-2. This report extends these previous studies by analyzing the margins to Onset of Nucleate Boiling (ONB) for these two DDEs under the conservative conditions used in the previous thermal-hydraulics analyses.

# 2. PROBLEM DESCRIPTION

The current section describes the geometry, boundary conditions, and material properties used for the analyses of the MITR and NBSR DDE.

## 2.1 NBSR GEOMETRY

The CAD-based geometry provided by SCK CEN and dimensions of the MITR and NBSR DDEs are depicted in Figure 1 and Figure 2, respectively.

The *MITR DDE* consists of a top coupling basket, bottom coupling basket, and the DDE basket that contains the fuel assembly. The upper panel of Figure 1 shows the three components assembled. The length of fuel plate is 23 inches. There are three types of plate that have different thickness of fuel core as depicted in Figure 2. Plates 1 and 19 employ Type-T fuel core with 0.013-inch thickness, plates 2, 3,17, and 18 employ Type-Y fuel core with 0.017-inch thickness, and plates 4-16 employ Type-F fuel core with 0.025-inch thickness. Following the CAD specifications, the width and length of fuel core in this report are 2.166 inches and 22.75 inches, respectively.

The *NBSR DDE* consists also of a top coupling basket, bottom coupling basket, and the DDE basket which contains the fuel assembly as shown in Figure 2. The NBSR consists of 34 fuel plates, 17 in the top set and 17 in the bottom set with 18 cooling channels between plates. These 17 top and bottom plates are swaged into grooves in the side plates. In Figure 2 the purple plates (named outer plates) are unfueled aluminum plates that extend the length of the assembly, while the grey are fuel plates. Each fuel plate consists of a 11.625 in fueled region length with additional clad extending on the top (1 in) and bottom (0.375 in) of each plate. The shorter span of clad is towards the midplane of the core to limit parasitic absorption of neutrons.

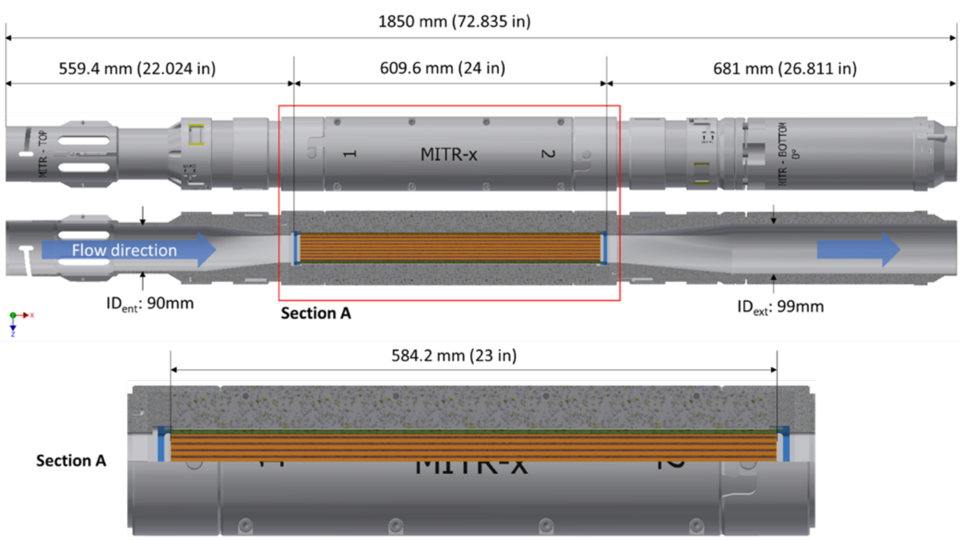

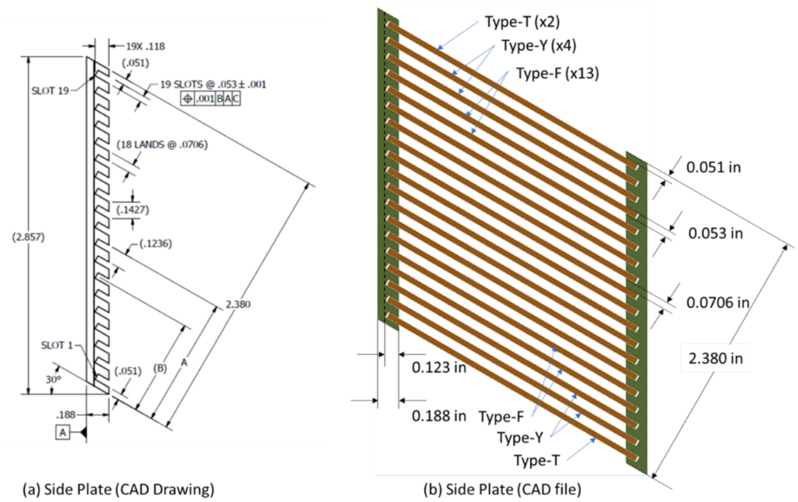


Figure 1. *MITR DDE* basket and fuel assembly. Top: Axial cut showing the basket and fuel assemblies key dimensions. Bottom: Detail of the fuel plates configuration.

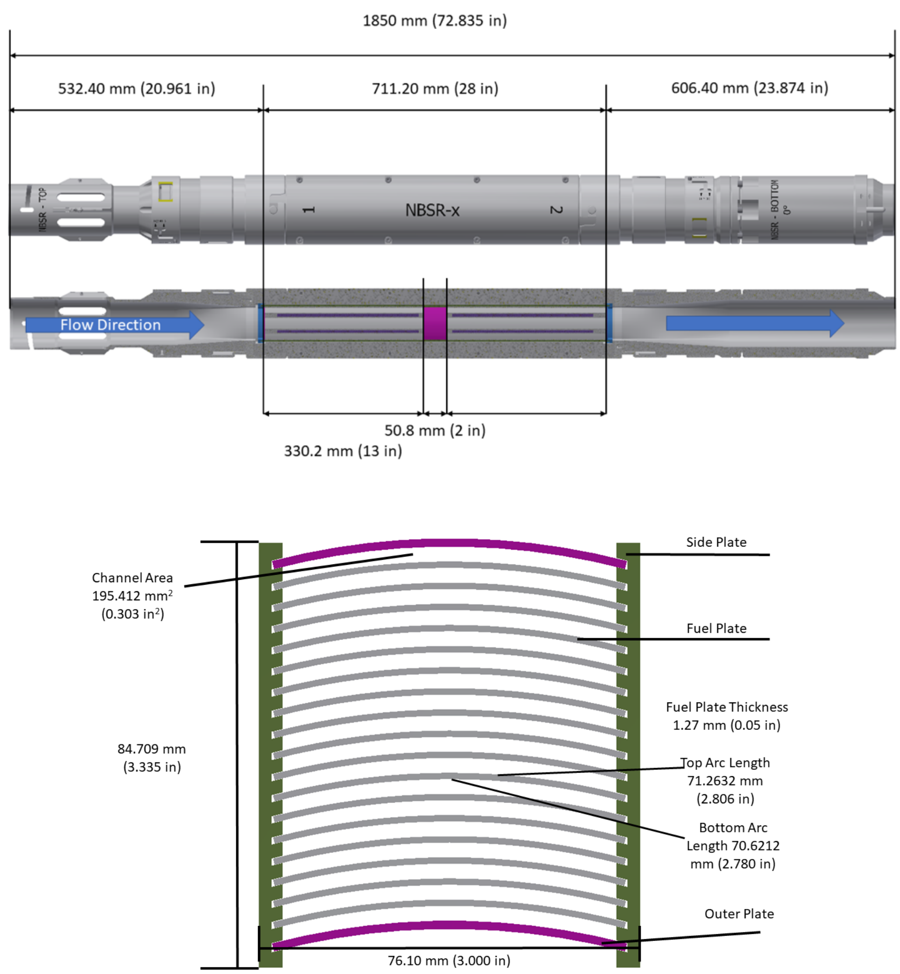


Figure 2. *NBSR DDE* basket and fuel assembly. Top: Axial cut showing the basket and fuel assemblies key dimensions. Bottom: Detail of the fuel plates configuration.

## 2.2 BOUNDARY CONDITIONS

The power density distributions of the MITR and NBSR DDEs during the first and second irradiation campaigns have been provided from SCK CEN [Kalcheva, 2022] and are presented in Table 1 and Table 2, respectively. There are 8 irradiation cycles for the MITR DDE and10 irradiation cycles for the NBSR one. The power density at each Beginning of Cycle (BOC) is provided for each case and, for all cases, it is considered that the power density remains constant and equal to that at the BOC.

For the *MITR DDE*, the peak power density provided for plate 16 is used for plates 1 through 16, the power density provided for plate 18 is used for the plates 17 and 18, and the power density provided for plate 19 is only used for plate 19 only. This assumption provides a bounding estimate as the peak plate power is significantly higher than the average one. Power is considered uniform in the transverse and axial directions for each plate.

For the *NBSR DDE*, three azimuthal discretizations were provided for the highest-power plate. This power was applied to all plates in the irradiation campaign. This provides a bounding case for the calculation as this power is substantially higher than true distribution. The reason the data starts at BOC-6 is because the irradiation campaign begins at BOC-1 with the MITR assembly and then at BOC-6 the NBSR assembly is also placed into the BR2 core. The axial power density is assumed uniform throughout analysis in this study. A uniform power distribution is also considered in the azimuthal direction as RELAP5-3D is not able to capture transverse heat conduction in version 4.4.2.

Table 1. Power Density calculated and assumed in *MITR DDE* fuel plates during the irradiation campaigns, the cycle time of each cycle was 31.5 days and the power during each irradiation campaign is assumed constant and equal to the Beginning of Cycle (BOC) power.

| Irradiation Campaign | MITR-Al-basket & Al-plug (12 Hf-rods) | | | |
|---|---|---|---|---|
| | Power Density (kW/cm$^3$) | | | |
| | Power Modeled for Plate | 1-16 | 17-18 | 19 |
| | Actual Plate for Power Reference | 16 | 18 | 19 |
| 1st standalone irradiation of MITR-DDE in position H5 | BOC 1, Power = 55 MW | 1.87 | 2.77 | 3.8 |
| | BOC 2, Power = 56 MW | 1.84 | 2.66 | 3.62 |
| | BOC 3, Power = 56 MW | 1.84 | 2.71 | 3.57 |
| | BOC 4, Power = 56 MW | 1.83 | 2.69 | 3.52 |
| | BOC 5, Power = 56 MW | 1.83 | 2.58 | 3.23 |
| 2nd simultaneous irradiation of MITR-DDE in position H5 and NBSR-DDE in position H3 | BOC 6, Power = 56 MW | 2.94 | 3.90 | 4.55 |
| | BOC 7, Power = 56 MW | 2.95 | 3.65 | 4.34 |
| | BOC 8, Power = 56 MW | 2.82 | 3.56 | 3.93 |
| EOL-MITR-DDE | End of Cycle 8 = EOL for MITR DDE | | | |

Table 2. Power Density calculated and assumed in *NBSR DDE* fuel plates during the irradiation campaigns, the cycle time of each cycle was 31.5 days and the power during each irradiation campaign is assumed constant and equal to the Beginning of Cycle (BOC) power.

| Irradiation Campaign | NBSR-Al-basket & Al-plug (12 Hf-rods) | | | |
|---|---|---|---|---|
| | Power Density ($kW/cm^3$) | | | |
| | Azimuth | 1st | 2nd | 3rd |
| 1st standalone irradiation of NBSR-DDE in position H5 | BOC 6, Power = 56 MW | 12.21 | 11.36 | 12.86 |
| | BOC 7, Power = 56 MW | 10.64 | 10.05 | 11.19 |
| | BOC 8, Power = 56 MW | 9.48 | 9.04 | 10.07 |
| 2nd simultaneous irradiation of NBSR-DDE in position H5 and NBSR-DDE in position H3 | BOC 9, Power = 60 MW | 9.04 | 8.76 | 9.81 |
| | BOC 10, Power = 60 MW | 8.09 | 7.73 | 8.62 |
| | BOC 11, Power = 60 MW | 6.93 | 6.67 | 7.26 |
| | BOC 12, Power = 60 MW | 6.08 | 5.89 | 6.54 |
| | BOC 13, Power = 60 MW | 5.18 | 5.17 | 5.47 |
| | BOC 14, Power = 60 MW | 4.83 | 4.84 | 5.14 |
| | BOC 15, Power = 60 MW | 4.10 | 3.87 | 4.38 |
| EOL-NBSR-DDE | End of Cycle 15 = EOL for NBSR DDE | | | |

The nominal average channel velocity of **MITR DDE** [Bert, 2022] s 2.6 m/s. The nominal channel velocity is the flow velocity at cross-section of fuel region where the flow area is 2213 $mm^2$. The frontal area of the inlet plenum duct in the CFD model is 6292.58 $mm^2$ according to the CAD model. The inlet velocity in the inlet plenum calculated by mass conservation to be 0.91434 m/s.

The nominal average channel velocity of **NBSR DDE** [Bert, 2022] s 6.6 m/s. The nominal channel velocity is the flow velocity at cross-section of fuel region where the flow area is 3520.56 $mm^2$. The frontal area of the inlet plenum duct in the CFD model is 6361.70 $mm^2$ according to the CAD model. The inlet velocity in the inlet plenum calculated by mass conservation to be 3.65 m/s.

For both cases, the pressure outlet boundary is specified by 0 Pa gauge pressure, while the operating pressure is set at 1.2 MPa. The inlet temperature into the domain is 308.15 K, whereas free convection boundary conditions are imposed in the outlet section of the domain.

## 2.3 MATERIAL PROPERTIES

The built-in IAPWS-IF97 water properties were adopted to specify the density, viscosity, thermal conductivity, specific heat, and dynamic viscosity of working fluid. IAPWS-IF97 is a temperature- and pressure-dependent water property. The temperature dependent density, specific heat, and thermal-conductivity for the U-10Mo fuel [Rabin et al., 2017] and Aluminum 6061 cladding [Polkinghorne & Lacy, 1991] are provided in Table 3. The thermal diffusivity of the Zirconium liner between the fuel and the cladding is neglected.

Table 3. Thermophysical properties for fuel and cladding materials.

| Material | Property | Equation | Temperature Validity Range |
|---|---|---|---|
| U-10Mo | Density [kg/m$^3$] | $\rho = -0.9215T[K] + 17409.0$ | [293,623] K |
| | Specific Heat [J/(kg.K)] | $C_P = 0.0692T[K] + 113.61$ | [293,623] K |
| | Thermal Conductivity [W/(m/K)] | $k = 0.0413T[K] + 0.1621$ | [293,1073] K |
| Aluminum 6061 | Density [kg/m$^3$] | $\rho = 2702.0$ | [293,573] K |
| | Specific Heat [J/(kg.K)] | $C_P = 3.97 \times 10^{-5}T[K]^2 + 0.41T[K] + 773.0$ | [298,805] K |
| | Thermal Conductivity [W/(m/K)] | $k = -1.73 \times 10^{-7}T[K]^3 + 2.66 \times 10^{-5}T[K]^2 + 0.16T[K] + 120.6$ | [298,811] K |

# 3. MODELS

The section summarizes the modeling approaches used for studying the thermal hydraulics, emphasizing on ONB.

## 3.1 RELAP5-3D THERMAL-HYDRAULICS MODEL

Thermal-hydraulics calculations are performed with RELAP5-3D (version 4.4.2). For validation of RELAP5-3D for this type of simulations we refer the reader to the references of this report [Miller & Shumway, 1992; Sloan et al., 1994; Weaver et al., 2002; Little, 2016; Maddock, 2017; RELAP5-3D, 2018; Narcisi et al., 2019; Collins, 2020; Martin & Williams, 2022].

The nodal diagrams for the *MITR* and *NBSR DDE* models are presented in Figure 3. In both models, the varying hydraulic diameter pipe and channels between plates are discretized using pipe components. The inlet and outlet fittings of the flow assembly are represented via branch components. For the NBSR DDE, the middle gap between the top and bottom set of plates is modeled via a branch component. The flow in both cases is imposed via a time dependent junction and the inlet temperature and outlet pressure via an inlet and outlet time dependent volume, respectively. Four channels are used in the MITR model, explicitly resolving channels 1-3 and lumping together channels 4-20. Similarly, a 3-channel model is used for the top and bottom set of plates of the NBSR DDE, where a top and bottom side channel and the adjacent subchannel are modeled explicitly and the remaining 16 channels are lumped together into one channel. The plates are modeled via heat structure, applying power only at the core of the fueled plates. Conjugate heat transfer boundary conditions are used for the plates in contact with channels, while a symmetry boundary condition is used for the right side of the average plate in contact with the average subchannel and the left side of the left side-plates. More details about the modeling approach can be found in the references. We refer the reader to [Tano & Yoon, 2022] for details about the MITR model and to [Tano & Mueller, 2022] for details about the NBSR one.

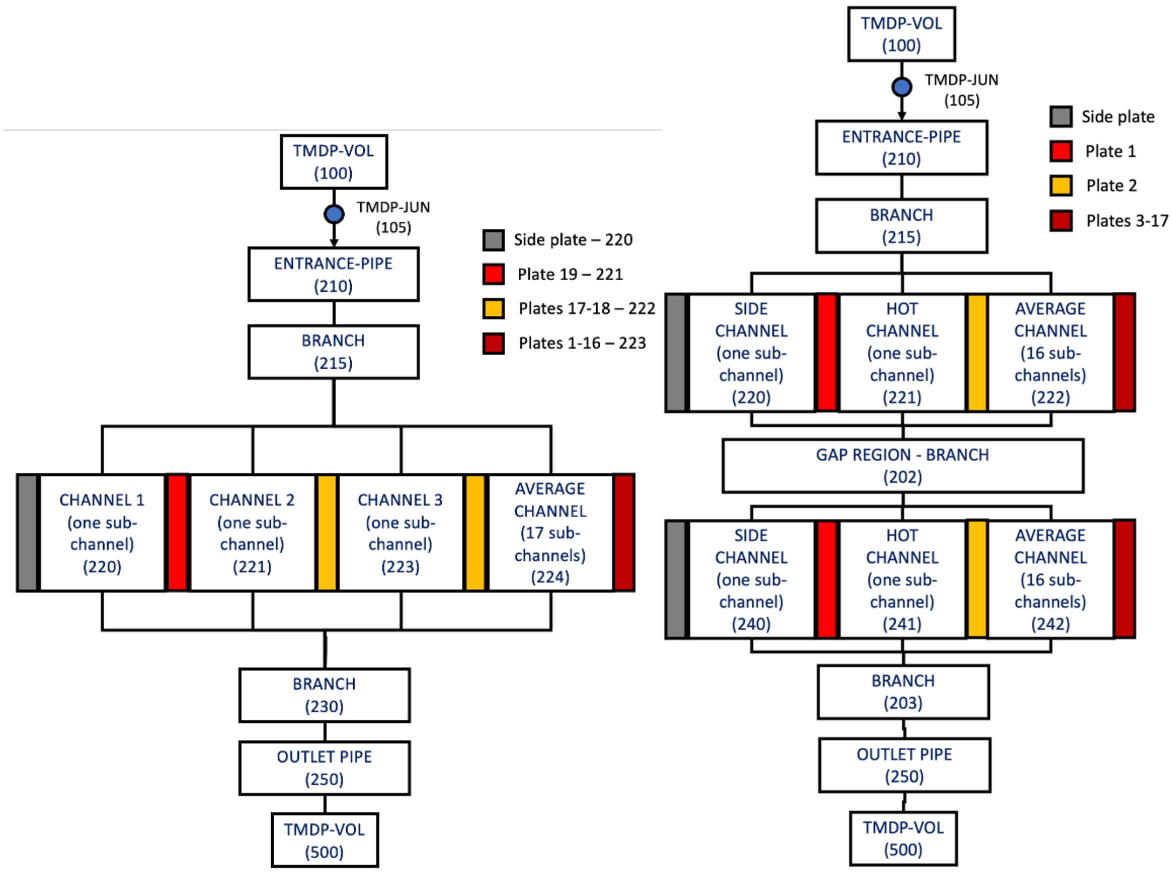


Figure 3. Nodal diagram for the RELAP5-3D MITR (left) NBSR(right) models.

## 3.2 ONSET OF NUCLEATE BOILING MODELS

The ONB models are implemented in RELAP5-3D as a post-processor using its Python bindings. This means that once the temperature at the plate surface ($T_w$) has been computed for all BOC configurations, the temperature margin to ONB is evaluated. Two different models have been implemented to study the margin to ONB. The Bergles and Rosenhow [Bergles & Rosenhow, 1964] model and the Satō and Mastsumura one [Satō & Mastsumura, 1964]. Both models have been observed to hold well under surface oxidation conditions (within a 25% of uncertainty) [Forrest et al., 2016] and are briefly described in the next subsections.

### 3.2.1 BERGLES AND ROSENHOW MODEL

Bergles and Rohsenow treat the bubble shape as hemispherical, noting that, for a hydrophilic surface, ONB occurs when the bubble equilibrium radius is equivalent to the critical bubble radius for the coolant and the surface. The model assumes that the bubble will grow when the superheat requirement is met at the top of the hemispherical bubble, i.e., at a distance from the surface equal to the bubble radius. However, as acknowledged in the article, this likely represents an upper bound for the ONB flux as bubbles will grow due to heat transfer even is the superheat criterion is met closer to the surface than the critical radius. The model also assumes that an optimal cavity size for the bubbles to nucleate will be somewhere available over the plate surface, which is mostly observed in non-polished surfaces. Results of this model have been validated for ONB in pipe experiments. By using a graphical solution method, the following relation is obtained for the ONB heat flux:

$$q''_{ONB} = 1083P^{1.16}[1.8(T_w - T_{sat})]^{\frac{2.16}{P^{0.0234}}},$$

where $P$ is the coolant pressure, $T_w$ is the surface temperature, and $T_{sat}$ is the saturation temperature at the given pressure. All variables are in SI units, except for the pressure ($P$) that is in bar. The domain of validity for the pressure in this correlation is [1,138] bar. Again, the nominal operation pressure for the MITR and NBSR DDEs is 1.2 MPa = 12 bar.

To better interpret the model, we analyze the bounding cases. For instance, if the heat extracted from the plate goes to zero, then ONB directly occurs at the saturation temperature. As heat flux extracted from the plates increases, the wall temperature of the plate must be higher than the saturation temperature for the tip of the bubble to reach the superheat condition. Hence, ONB starts occurring at a plate temperature higher than the saturation one. In the limiting case where the heat flux goes to infinity, the model theoretically predicts no ONB as the wall temperature needs to be infinitely high for ONB to occur. This last case is evidently an example of the theoretical limitations of the model. Nonetheless, since the conditions for which this model has been validated resemble those of the current DDEs, it is appropriate to use of this model for ONB prediction.

In our case, to compute the temperature margin to ONB, we extract the wall temperature at which ONB will occur as follows:

$$T_w = \frac{1}{1.8}\left(\frac{q''_{ONB}}{1083P^{1.16}}\right)^{\frac{P^{0.0234}}{2.16}} + T_{sat},$$

Note that the pressure field next to the wall is part of the RELAP5-3D solution, while the heat flux is imposed via the set power densities in our model. Hence, we then define the temperature margin to ONB as follows:

$$\Delta T_{ONB,BR} = \left[\frac{1}{1.8}\left(\frac{q''_{ONB}}{1083P^{1.16}}\right)^{\frac{P^{0.0234}}{2.16}} + T_{sat}\right] - T_{w,RELAP},$$

where $T_{w,RELAP}$ is the wall temperature predicted by the RELAP5-3D model.

### 3.2.2 SATŌ AND MATSUMURA MODEL

One issue of the Bergles and Rosenhow model is that the plate temperature for ONB is independent of flow convection and the density difference between the liquid coolant and the vapor phase. Satō and Matsumura approach this issue by assuming a complete sphere (not a truncated sphere) sitting on the surface. Then, they select the full height of the spherical bubble as the required distance to meet the superheated condition. The thickness of the superheated layer is then defined solely by heat conduction in the liquid as follows:

$$\delta = \frac{k_l(T_w - T_{sat})}{q''_W},$$

where $k_l$ is the liquid thermal conductivity for the pressure and temperature next to the surface. This distance defines a quadratic equation for the radius of supported bubble sizes at which the bubble tip reaches the superheated condition. The ONB point is then defined as the minimum distance at which the bubble reaches the superheated condition, which yields an expression for the ONB heat flux as follows:

$$q''_{ONB} = \frac{k_l h_{fg}}{3\sigma T_{sat}\left(\frac{1}{\rho_v} - \frac{1}{\rho_l}\right)} (T_w - T_{sat})^2,$$

where $h_{fg}$ is the phase change enthalpy for the pressure next to the surface, $\sigma$ is the bubble surface tension, and $\rho_v$ and $\rho_l$ are the next-to-surface densities of vapor and liquid, respectively. All units for this expression are in SI units. Like in the Bergles and Rosenhow model, we can simplify out the wall temperature and define a margin to ONB as follows:

$$\Delta T_{ONB,SM} = \left[ T_{sat} + \sqrt{\frac{3\sigma T_{sat}\left(\frac{1}{\rho_v} - \frac{1}{\rho_l}\right) q''_{ONB}}{k_l h_{fg}}} \right] - T_{w,RELAP}.$$

# 4. STUDY RESULTS

The thermal-hydraulics fields and oxide layers thicknesses for all BOC configurations have been characterized in previous reports. See [Tano and Yoon, 2022] for MITR and [Tano and Mueller, 2022] for the NBSR. Hence, the results presented in this report deal exclusively with ONB.

The present section summarizes key results of the study. Previous validation work of comparing the RELAP5-3D and CFD simulations to validate the modeling hypotheses were done for the MITR DDE [Tano & Yoon, 2022]. The reader is referred to this report for details about this cross-validation approach. The non-isothermal pressure-drop, velocity profiles, temperature, and heat transfer coefficient distributions are studied for all BOC configurations; from BOC-6 to BOC-15. Next, the oxide growth over the plates is studied for all BOC configurations. Finally, the deformations and stress distributions over the plates are analyzed.

## 4.1 MARGINS TO ONB FOR THE *MITR* DDE

The maximum plate surface temperature predicted in the RELAP5-3D model is for the bottom region of the average plate and it is ~348 K. For comparison, the saturation temperature of water at the pressure operation condition of 1.2 MPa is 461.1 K. So, there would already be a margin of ~113.1 K for standard pool boiling conditions. The temperature margins to ONB for the discretized axial positions in the fuel plates and for all BOC configurations are depicted in Figure 4. It is observed that the temperature margins to ONB reduce for the bottom part of the plates. This is because this bottom part is hotter as the flow field heats up while it descends in the fuel assembly. The margins to ONB increases from BOC-1 to BOC-5 as the power density in the plates decreases. Then, margins suddenly reduce for BOC-6 because of the sudden power density increase for this configuration as the MITR DDE goes into its second irradiation campaign. The minimum margin to ONB is observed for the bottom part of the average plate for BOC-6 and it is ~115 K. The Bergles and Rosenhow model predict smaller temperature margins to ONB, which is in good agreement with the overconservativeness remarked for this model.

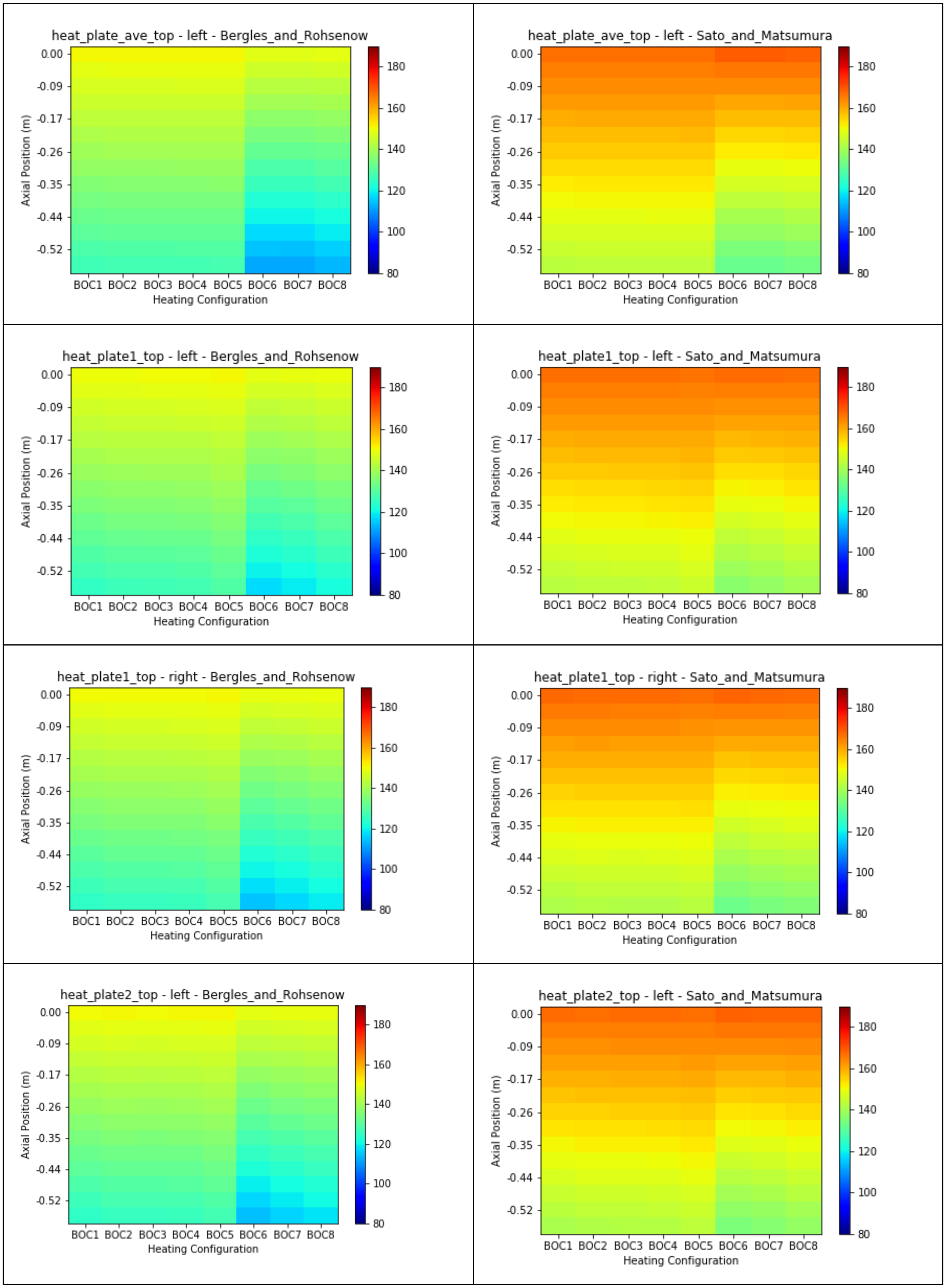
heat_plate_ave_top - left - Bergles_and_Rohsenow
heat_plate_ave_top - left - Sato_and_Matsumura
heat_plate1_top - left - Bergles_and_Rohsenow
heat_plate1_top - left - Sato_and_Matsumura
heat_plate1_top - right - Bergles_and_Rohsenow
heat_plate1_top - right - Sato_and_Matsumura
heat_plate2_top - left - Bergles_and_Rohsenow
heat_plate2_top - left - Sato_and_Matsumura
Axial Position (m)
0.00
-0.09
-0.17
-0.26
-0.35
-0.44
-0.52
BOC1 BOC2 BOC3 BOC4 BOC5 BOC6 BOC7 BOC8
Heating Configuration
180
160
140
120
100
80

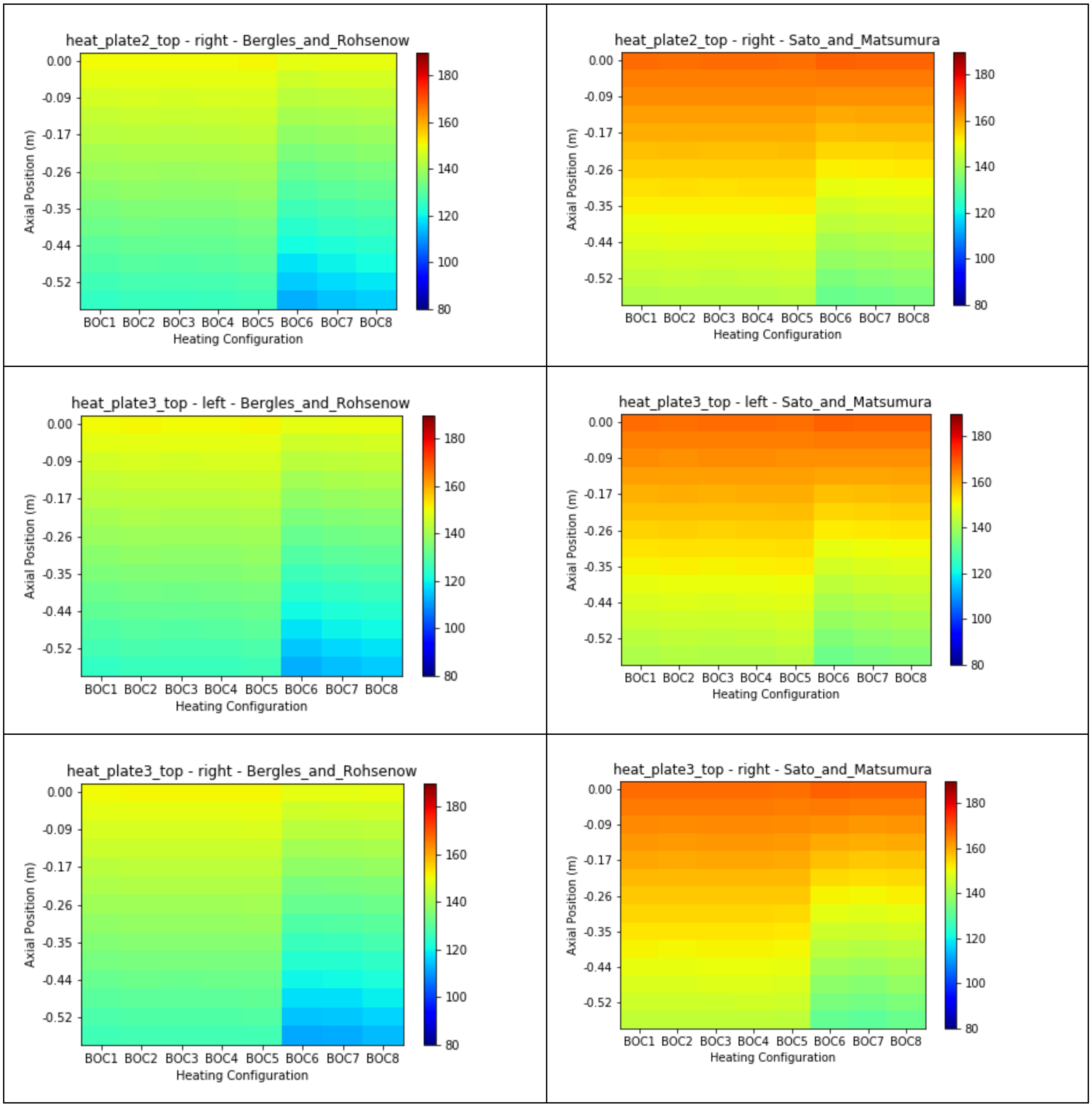


Figure 4. Temperatures margins [K] to ONB for the MITR DDE. Naming convention: <model plate number>_ <plate side {left, right}>_<ONB model name>

## 4.2 MARGINS TO ONB FOR THE *NBSR* DDE

The maximum plate surface temperature predicted in the RELAP5-3D model is for the bottom region of plate 2 in the bottom set of plates and it is ~349 K. Again, the saturation temperature of water at the operation condition of 1.2 MPa is 461.1 K. So, there would already be a margin of ~112.1 K for standard pool boiling conditions. The temperature margins to ONB for different axial positions in the fuel plates and for all BOC configurations are depicted in Figure 4 and Figure 5, for the top and bottom set of plates, respectively. The hottest temperatures are obtained at the bottom set of plates due to the descending flow.

Hence, the bottom set of plates have therefore smaller margins to ONB (minimum margin ~114 K) than the top ones (minimum margin ~138 K). As in the MITR case, the Bergles and Rosenhow model predicts smaller temperature margins to ONB due to the overconservativeness remarked for this model.

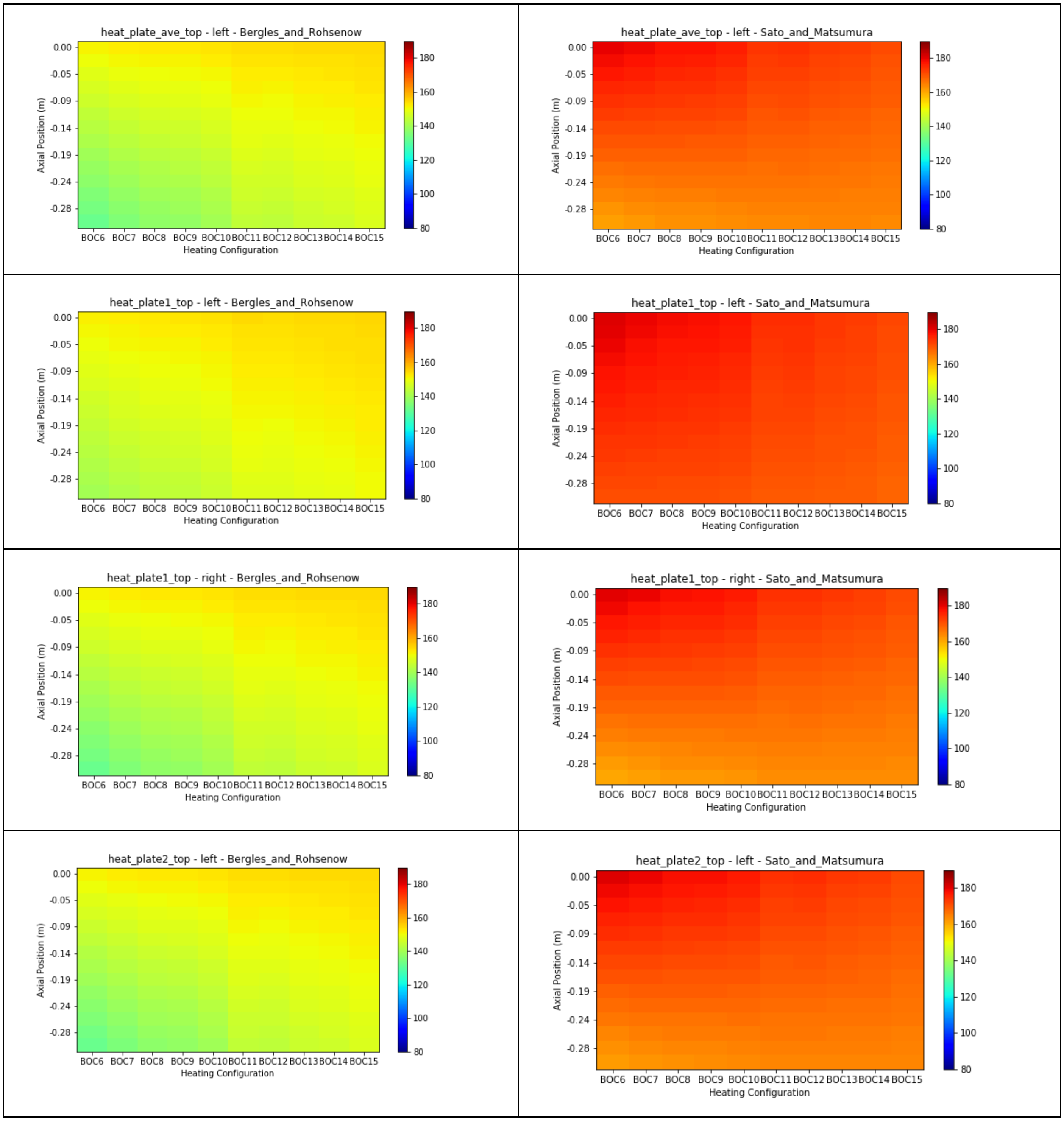

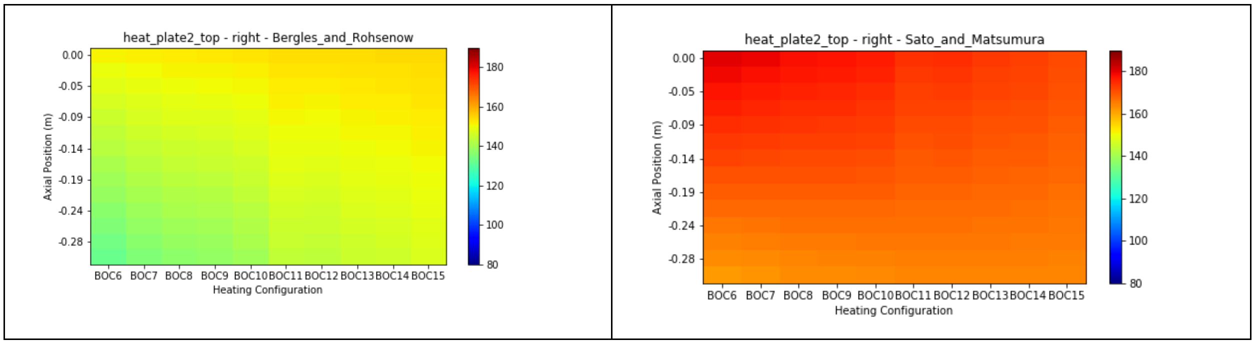


Figure 5. Temperatures margins [K] to ONB for the top fuel plate of the NBSR DDE. Naming convention: <model plate number> _<position (top, bottom)>_ <plate side {left, right}>_<ONB model name>

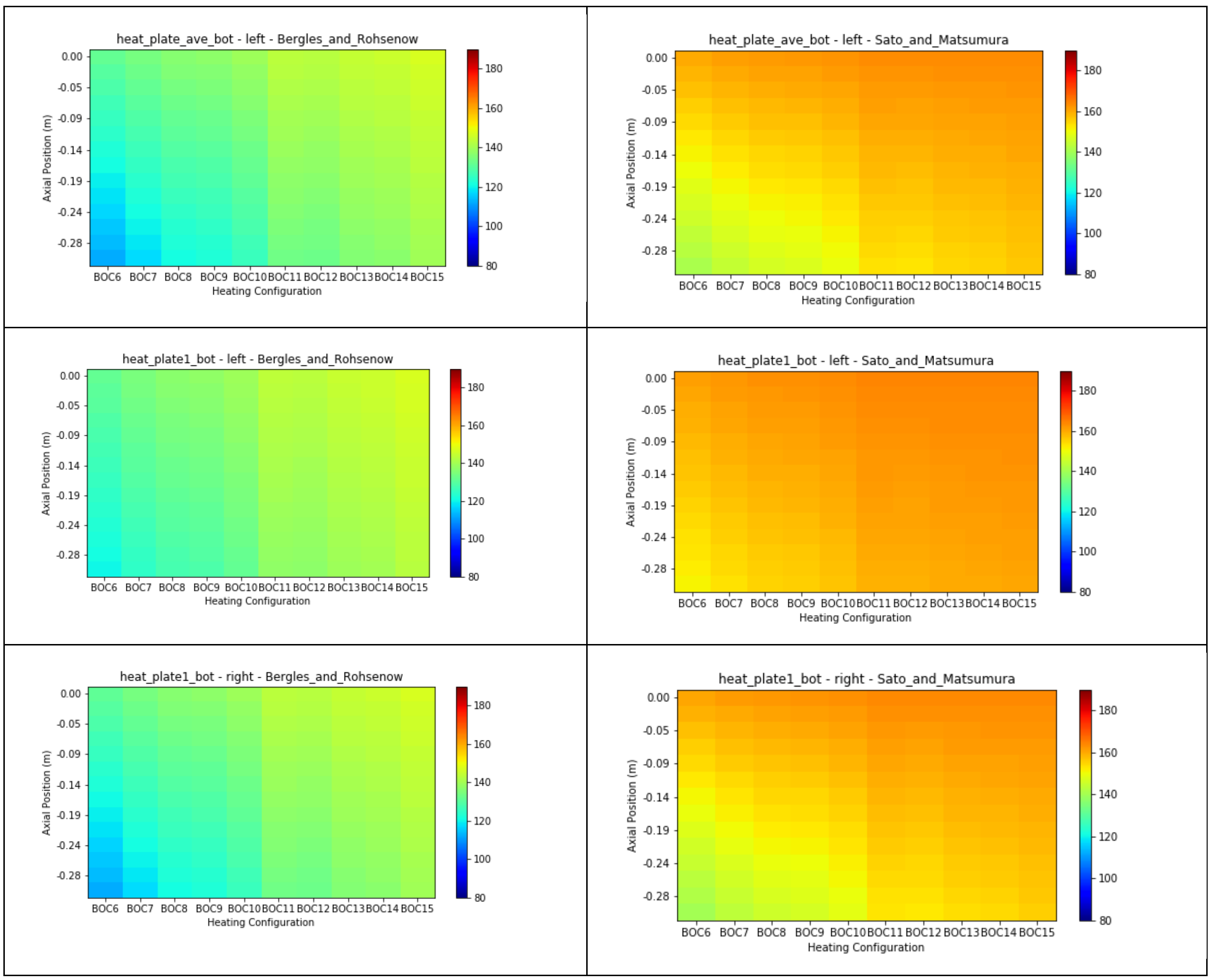

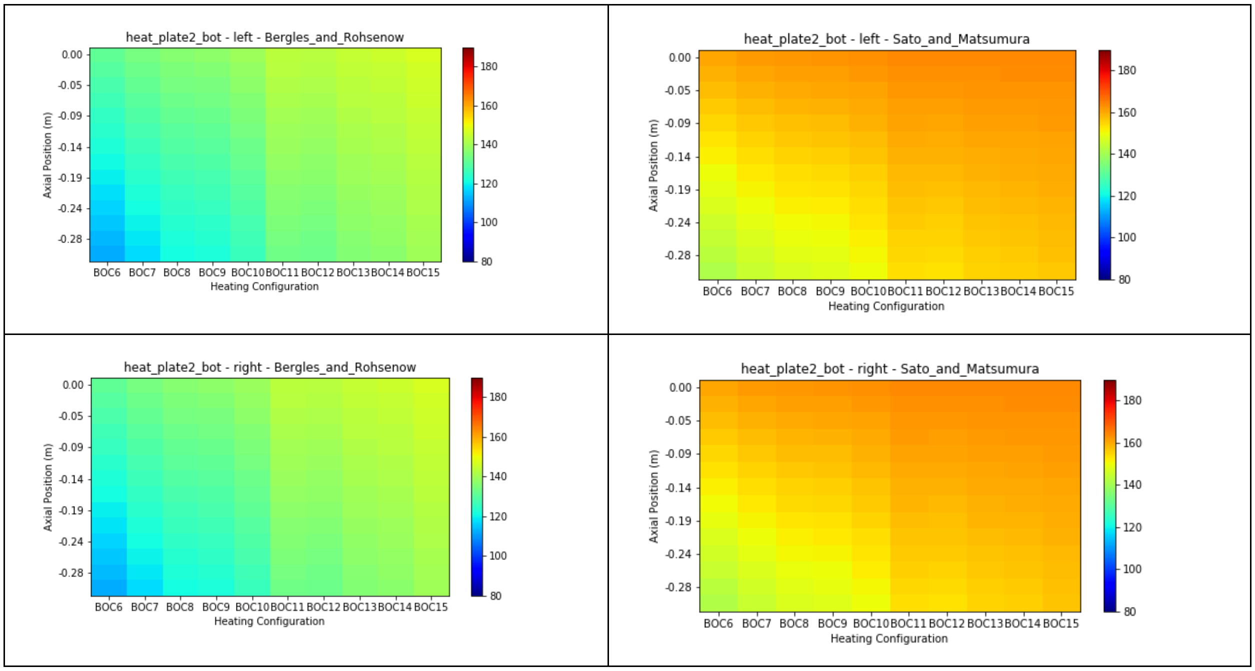


Figure 6. Temperatures margins [K] to ONB for the top fuel plate of the NBSR DDE. Naming convention: <model plate number> _<position (top, bottom)>_ <plate side {left, right}>_<ONB model name>

# 5. CONCLUSIONS

In this report the margins to ONB with a lumped parameters RELAP5-3D model have been studied for the MITR and NBSR DDEs. Conservative power densities have been applied to the fuel plates following the computed power densities during irradiation in the BR2. Two different models have been evaluated when predicting the ONB margins, the Bergles and Rosenhow model and the Satō and Matsumura one. Even though the Bergles and Rosenhow model is likely over-conservative, it predicts minimum margins to ONB of ~115 K and ~114 K for the MITR and NBSR experiments, respectively. Thus, we conclude that ONB is highly unlikely to pose an issue for the valuated conditions. Additionally, for the same coolant flow rates, ONB will also not be an issue if the power densities are kept equal or below to the conservative ones used in this study.

# 6. REFERENCE


Bergles, A.E. and Rohsenow, W.M., 1964, "The Determination of Forced-Convection Surface-Boiling Heat Transfer," Journal of Heat Transfer, 86, pp. 365-372. DOI: 10.1115/1.3688697.

Bryson, J. W., & Dickson, T. L. (1993). *Stress-intensity-factor influence coefficients for axial and circumferential flaws in reactor pressure vessels* (No. CONF-930702--4). Oak Ridge National Lab.

A. Collins, "VTR modeling and simulation using INL RELAP5 system code, ECAR-4788, 2020.

B. Rabin, M. Meyer, J. Cole, I. Glagolenko, G. Hofman, W. Jones, J. Jue, D. Keiser Jr, Y. Kim,C. Miller,et al., "Preliminary report on U-Mo monolithic fuel for research reactors", Idaho National Laboratory INL/EXT-17-40975, 2017.

B. Rossaert, "Briddes-mustang-r critical velocity analysis for NBSR and nsbr, calculation note-nc4986/n0brid-des/02/br", Restricted Contract Report SCK CEN/46944057 (R-8944), 2022.

C. Miller and R. Shumway, "Relap5/mod3 code quality assurance plan for ornl ans narrow channelflow and heat transfer correlations," EG and G Idaho, Inc., Idaho Falls, ID (United States), Tech.Rep., 1992.

Forrest, E. C., Don, S. M., Hu, L. W., Buongiorno, J., & McKrell, T. J. (2016). Effect of surface oxidation on the onset of nucleate boiling in a materials test reactor coolant channel. *Journal of Nuclear Engineering and Radiation Science*, *2*(2).

R. Little, "Results of Physics Calculations in Support of RELAP5 analysis of the enhanced LEU fuel(ELF) MK 1A,"ECAR-2469, 2016.

R. Martin and J. Williams, "Safety software evidence ranking for determining analytical readiness with a case study utilizing relap5-3d," 19th International Topical Meeting on Nuclear Reactor Thermal Hydraulics (NURETH-19), Mar. 2022.

RELAP5-3D Code Development Team, "Relap5-3d code manual. volume 4, models and correlations," Idaho National Laboratory, Tech. Rep., 2018.

Release notes for relap5-3d version 4.4.2.2021. [Online]. Available:https://relap53d.inl.gov/Shared%5C%20Documents/Release%5C%20Notes/Release%5C%20Notes%5C%20for%5C%20RELAP5%5C%204.4.2.pdf.

S. J. Pawel, D. K. Felde, and R. Pawer, "Influence of coolant ph on corrosion of 6061 aluminum under reactor heat transfer conditions,"ORNL/TM-13083, 1995. DOI:10.2172/205846. [Online].Available:https://digital.library.unt.edu/ark:/67531/metadc671895.

S. Polkinghorne and J. Lacy, "Thermophysical and Mechanical Properties of ATR Core Materials" EG&G Idaho Inc., Internal Technical Report, 1991.

S. Sloan, R. Schultz, and G. Wilson, "Relap5/mod3 code manual," EG and G Idaho, Inc., Idaho Falls,ID (United States). Idaho National ..., Tech. Rep., 1994

S. Kalcheva, "Feasibility study for dde-NBSR and nbsr irradiation in br2 november 2021 – ed01,"SCKCEN, Document BR2-RCE-RFA, Table XIX (NBSR DDE) and XX (NBSR DDE), 2021.

Satō, T. and Matsumura, H., 1964, "On the Conditions of Incipient Subcooled-Boiling with Forced Convection," Bulletin of the Japan Society of Mechanical Engineers, 7, pp. 329-398. DOI: 10.1299/jsme1958.7.392.

T. L. Maddock, "Results of Physics Calculations in Support of RELAP5 analysis of the enhanced LEU fuel (ELF) design", ECAR-2230, 2017.

Tano M. and Mueller C., "Preliminary NBSR Design Demonstration Element Thermal-Hydraulics and Structural analyses", INL/PRT-22-XXXXX, 2022

Tano M. and Yoon S.J., “Preliminary MITR Design Demonstration Element Thermal-Hydraulics and Structural analyses”, INL/PRT-22-XXXXX, 2022

V. Narcisi, P. Lorusso, F. Giannetti, A. Alfonsi, and G. Caruso, “Uncertainty quantification method for relap5-3d© using raven and application on nacie experiments, ”Annals of Nuclear Energy, vol. 127,pp. 419–432, 2019.

W. L. Weaver, E. Tomlinson, and D. Aumiller, “A generic semi-implicit coupling methodology for use in relap5-3d©,”Nuclear Engineering and Design, vol. 211, no. 1, pp. 13–26, 2002.